

Coefficient of restitution for one-dimensional harmonic solids

Anthony G. Basile

Department of Math and Natural Sciences, D'Youville College, Buffalo, New York 14201-1084

Randall S. Dumont

Department of Chemistry, McMaster University, Hamilton, Ontario, Canada L8S 4M1

(Received 18 June 1999)

Using a numerical algorithm based on the time evolution of normal modes, we calculate the coefficient of restitution η for various one-dimensional harmonic solids colliding with a hard wall. We find that, for a homogeneous chain, $\eta=1$ in the thermodynamic limit. However, for a chain in which weaker springs are introduced in the colliding front half, η remains significantly less than one even in the thermodynamic limit, and the “lost” energy goes mostly into low frequency normal modes. An understanding of these results is given in terms of how the energy is redistributed among the normal modes as the chain collides with the wall. We then contrast these results with those for collisions of one-dimensional harmonic solids with a soft wall. Using perturbation theory, we find that $\eta=1$ for all harmonic chains in the extremely soft wall limit, but that inelasticity grows with increasing chain size in contrast to hard wall collisions.

PACS number(s): 45.10.-b, 45.50.Tn

I. INTRODUCTION

Collisions have long been studied in physics and the development of their dynamics has led to the formulation of numerous conservation laws. Historically, the conservation of energy remained elusive because it holds only for systems in which conservative forces act; yet, most macroscopic systems have some dissipative forces at work and so tend to “loose” energy with time. Nonetheless, at the microscopic level, the forces holding ordinary matter together are electromagnetic in nature and therefore conservative. Dissipation is then understood as energy which was originally in a few macroscopic degrees of freedom, but which *somehow* gets diffused among many microscopic degrees of freedom as the interaction progresses. However, while it is easy to understand how conservative forces conserve energy, it is not so easy to see how they can dissipate it.

Recent studies of the scattering of thermal clusters from solid surfaces raise such questions [1–4]. These studies focus on collisions with significant deposition of translational kinetic energy into internal modes, and concern themselves with collision-activated energy-threshold processes, such as chemical reactions of species imbedded in inert clusters, or cluster evaporation and shattering. In connection to these studies, in this paper we investigate the more elementary question of the dynamical mechanism for internal energy deposition, without the complications associated with (a) initial internal energy, (b) activation of threshold processes, and (c) interactions between rotational and vibrational degrees of freedom. To this end, we consider the coefficient of restitution of one dimensional harmonic solids initially at 0 K.

The literature’s treatment of the coefficient of restitution is largely concerned with collisions of macroscopic bodies. In particular, there is a focus on the role of rotational dynamics, to the extent that some studies consider only rigid body collisions [5]. In general, there is a reliance on simulation based on a phenomenological description of the interaction between small elements within the colliding bodies which include intrinsically dissipative forces [6]. In contrast to

these studies, our approach here is to focus solely on conservative translational to vibrational energy transfer, as a model for low energy microscopic cluster collisions.

The coefficient of restitution is introduced to measure the translational kinetic energy “lost” during a collision:

$$\eta = \frac{K_a}{K_b}, \quad (1)$$

where K_b and K_a are the translational kinetic energies before and after the collision, respectively. Succinctly put then, our question is this: If one maintains that at a sufficiently microscopic level the forces holding the solid together are conservative, then no energy is lost during the collision and the difference, $K_b - K_a$, must go into the internal degrees of freedom of the elastic solid. What internal degrees of freedom are excited and how are they excited? Below, we address this question by considering the dynamics of one dimensional solids of identical point masses connected by harmonic springs which are made to collide with a hard or soft wall. While this model represents a strong idealization of real physical systems—in particular, it is one dimensional and only takes into account harmonic interactions—it does yield exact analytical solutions and so makes explicit at least one mechanism for the dissipation of energy by conservative forces.

Since our aim is to gain insight into how η varies with the internal structure of the solid, we first investigate an ideal case in which $\eta=1$ and then see how deviation from it can lead to $\eta<1$. We show that the homogeneous chain, in which all the spring constants are equal [7], has $\eta=1$ in the thermodynamic limit when it collides with a hard wall, while the introduction of a “cushion” in the form of weaker springs placed in the colliding front half of the chain generally leads to $\eta<1$. Augmenting our numerical study with a heuristic analysis, we argue why this should be the case and arrive at some intuitive understanding of a mechanism by which energy can be dissipated by conservative forces. We then contrast hard wall collisions with soft wall collisions

and conclude from our analysis that (1) all harmonic chains have $\eta=1$ in the adiabatic (extremely soft wall) limit and that (2) inelasticity grows with increasing chain size, which is the opposite of hard wall collisions.

The remainder of this paper is organized as follows. In Sec. II, we present the details of our model for hard wall collisions and derive a method for solving its dynamics by time evolving the normal modes. In Sec. III, we present our results for the homogeneous chain and give a heuristic analysis of why $\eta=1$ in the thermodynamic limit. In Sec. IV, we treat the cushioned chain and, in light of what was found in Sec. III, argue for how $\eta<1$ is obtained. In Sec. V, we present our model for soft wall collisions and argue why $\eta=1$ in the adiabatic limit, with inelasticity growing with increasing chain size. Finally, we close with some general remarks.

II. NORMAL MODE DYNAMICS OF ONE-DIMENSIONAL HARMONIC SOLIDS: HARD WALL COLLISIONS

The Hamiltonian for a one dimensional harmonic solid of n identical point masses, interacting with a hard wall, can be written as

$$H = H_0 + H_I, \quad (2)$$

where H_0 represents the interaction of the point masses with one another and H_I represents the interaction of the chain with the hard wall. The first term is given by

$$H_0 = \frac{m}{2} \sum_{i=1}^n \dot{x}_i^2 + \frac{1}{2} \sum_{i=1}^{n-1} k_i (x_{i+1} - x_i - a)^2, \quad (3)$$

where m , x_i , and \dot{x}_i are the mass, position, and velocity of particle i , respectively. Particles i and $i+1$ interact via a harmonic potential with spring constant, k_i , and have an equilibrium spacing, a . The interaction with the hard wall at $x=0$ can be accounted for by letting $\dot{x}_1 \rightarrow -\dot{x}_1$ whenever $x_1=0$. The effect of H_I on the equations of motion is given below, but we note here that H_I does not change the total energy of the system, and so incorporates no dissipative terms into Eq. (2).

Next, we define the homogeneous limit of Eq. (3) as the case where $k_i=k$, for all i . The thermodynamic limit can then be understood as $n \rightarrow \infty$, with $M=nm$, $K=k/n$, and $A=na$ fixed. These relations guarantee that the mass M , spring constant K , and length A of the entire chain will remain finite as the limit is taken. The homogeneous chain can now be modified by letting some of the k_i differ from one another. In this case, it is still possible to keep the overall spring constant of the chain fixed in the thermodynamic limit by insisting that $K=1/\sum_{i=1}^{n-1} (1/k_i)$ remain fixed.

In the absence of H_I , the equations of motion can be obtained from Eq. (3) via the Hamiltonian formalism which, in matrix language, gives

$$\ddot{\mathbf{y}} = -\mathbf{K}\mathbf{y}, \quad (4)$$

where $y_i = x_i - (i-1)a$, for $i=1, 2, \dots, n$, and \mathbf{K} is a tridiagonal matrix which depends on the k_i 's and m . Eq. (4) can be solved by a normal mode decomposition in which \mathbf{K} is

diagonalized. Numerically, since \mathbf{K} is a symmetric tridiagonal matrix, its diagonalization (eigenvalues plus eigenvectors) entails an order n^2 operation which, in the homogeneous limit, reduces to simple analytical expressions. Taking the eigenvalues and eigenvectors to be ω_j^2 and \hat{e}_j , respectively, with $j=1, 2, \dots, n$ labeling the normal modes, we can write

$$\vec{y}(t) = \sum_{j=1}^n \alpha_j(t) \hat{e}_j, \quad (5)$$

where $\alpha_j(t)$ obeys $\ddot{\alpha}_j(t) + \omega_j^2 \alpha_j(t) = 0$, and has solution,

$$\alpha_j(t) = \text{Re} \left[\frac{C_j}{\omega_j} \exp(-i\omega_j t) \right]. \quad (6)$$

Here $C_j = \omega_j A_j + iB_j$, where A_j and B_j are real constants independent of time. Written in this form, Eq. (6) holds even for the center of mass (c.m.) mode, $j=1$, provided one treats $\omega_1 \rightarrow 0^+$ as a limit. Eq. (3) can now be written as $E_0 = \sum_{j=1}^n E_j$, where the energy in mode j is given by

$$E_j = \frac{1}{2} m C_j C_j^*, \quad (7)$$

and is independent of time. Recalling that the above was derived in the absence of any interaction with the hard wall, a nice interpretation now arises. The energy in any particular normal mode remains constant during the time between collisions of particle $i=1$ with the wall. However, once such a collision does occur, the total energy of the system does not change, but its distribution among the normal modes does. The question of how energy in a macroscopic degree of freedom is ‘‘lost’’ to the many microscopic internal degrees of freedom reduces, for our model, to an investigation into how the energy gets redistributed among the normal modes as the collision progresses.

The interaction of particle $i=1$ with the hard wall can now be added by modeling the impulse given by the wall to the particle with a delta function force. Suppose particle $i=1$ collides with the wall at times $t=t_1, t_2, t_3, \dots$. If immediately before the p th collision this particle has velocity $\dot{x}_1(t_p^-)$, then immediately after, it has velocity $v_p = \dot{x}_1(t_p^+) = -\dot{x}_1(t_p^-)$, and the force exerted by the wall is given by $F_p = 2m v_p \delta(t - t_p)$. This changes the equation of motion for particle $i=1$ in Eq. (4), the other components being unaffected, and gives

$$\ddot{\mathbf{y}} = -\mathbf{K}\mathbf{y} + 2\hat{g} \sum_p v_p \delta(t - t_p), \quad (8)$$

where the sum is over all the collisions that particle $i=1$ makes with the hard wall, and $\hat{g} = (1, 0, 0, \dots, 0)$. Restricting ourselves to a sufficiently small neighborhood of $t=t_p$, $\alpha_j(t)$ now obeys $\ddot{\alpha}_j(t) + \omega_j^2 \alpha_j(t) = 2(\hat{g} \cdot \hat{e}_j) v_p \delta(t - t_p)$, and has the solution

$$\alpha_j(t) = \text{Re} \left[\frac{C_j^{(p-1)}}{\omega_j} \exp[-i\omega_j(t - t_{p-1})] \right], \quad (9)$$

for $t_{p-1} < t < t_p$, and

$$\alpha_j(t) = \text{Re} \left[\frac{C_j^{(p-1)}}{\omega_j} \exp[-i\omega_j(t-t_{p-1})] + \frac{2i\nu_p(\hat{g} \cdot \hat{e}_j)}{\omega_j} \right. \\ \left. \times \exp[-i\omega_j(t-t_p)] \right], \quad (10)$$

for $t_p < t < t_{p+1}$. If we take Eq. (9) as the standard form for expressing $\alpha_j(t)$ in terms of C_j , then a mapping is suggested which connects the value of C_j before the p th collision, $C_j^{(p-1)}$, to its value after, $C_j^{(p)}$:

$$C_j^{(p)} = C_j^{(p-1)} \exp(-i\omega_j \Delta t_{p-1}) + 2i\nu_p(\hat{g} \cdot \hat{e}_j), \quad (11)$$

where $\Delta t_{p-1} = t_p - t_{p-1}$ is the time the system takes to evolve from the $(p-1)$ th to the p th collision. The terms in Eq. (11) are easily understood. The first term arises because we update the reference time in Eq. (9) from t_{p-1} to t_p with each successive collision—it represents the advance in the phase of $C_j^{(p-1)}$. But the second term is the boost given to the velocity by the collision. Unfortunately, to apply Eq. (11) numerically requires not only the value of $C_j^{(p-1)}$, but also Δt_{p-1} and ν_p , which we do not have *a priori*. At least ν_p can be expressed in terms of $C_j^{(p-1)}$ using

$$\nu_p = -\dot{x}_1(t_p^-) = -\text{Im} \left[\sum_{j=1}^n (\hat{g} \cdot \hat{e}_j) C_j^{(p-1)} \exp(-i\omega_j \Delta t_{p-1}) \right]. \quad (12)$$

But, Δt_{p-1} has no simple expression [8], and must be obtained as the solution to

$$y_1(t_p) = \text{Re} \left[\sum_{j=1}^n \frac{(\hat{g} \cdot \hat{e}_j) C_j^{(p-1)}}{\omega_j} \exp(-i\omega_j \Delta t_{p-1}) \right] = 0. \quad (13)$$

A simple bracketing technique is sufficient to find the zero since the approximate value of Δt_{p-1} is known, as will be discussed in the next section.

Now, only the initial conditions in Eq. (11) need to be specified, and then the entire dynamics of the chain can be found by repeatedly applying the above mapping. The initial value of $C_j^{(0)}$ can be expressed in terms of the initial positions and velocities of the particles $A_j^{(0)} = \vec{y}(0) \cdot \hat{e}_j$, $B_j^{(0)} = \vec{y}'(0) \cdot \hat{e}_j$. If we initialize the chain at $t_0 = 0$ with all its energy in the c.m. mode, that is, with $y_i(0) = 0$, and $\dot{y}_i(0) = -v_c$, then $C_j^{(0)} = -i\nu_c \sqrt{n}$ for $j = 1$, and zero otherwise.

We checked the above algorithm against molecular dynamics. The Euler-Cromer algorithm is both fast and accurate for this system [9]. Using a time step, $\Delta t = (0.001)\sqrt{m/k}$, we find that the energy of the system is constant within an error margin of at most 0.05% for various $n = 100$ chains—both homogeneous and not. Although both molecular and normal mode dynamics involve an order n^2 operation to find η , and both lead to comparable results, the latter is faster by a factor of about 20 and more accurate. Error propagation occurs in molecular dynamics because of the unavoidable finite time step; whereas, every calculation in normal mode dynamics can essentially be reduced to machine accuracy.

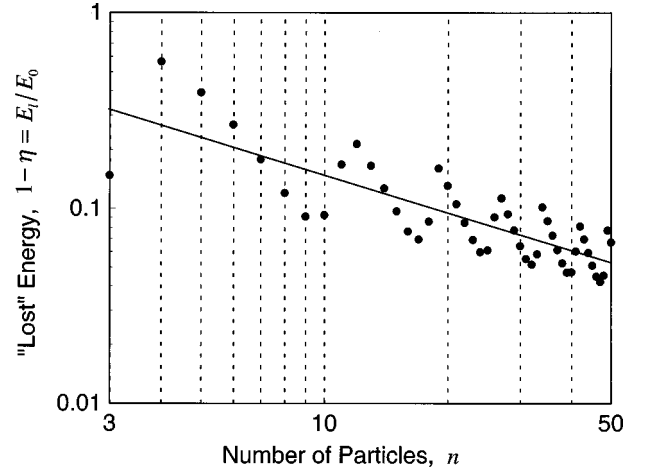


FIG. 1. The deviation of η from unity as a function of chain size for the homogeneous chain.

III. RESULTS FOR THE HOMOGENEOUS CHAIN: HARD WALL COLLISIONS

For our numerical work, we take the mass, length, and time scale to be m , a , and a/v_c , respectively. (This amounts to setting $m = a = v_c = 1$ in our equations; however, to avoid ambiguity, we leave these parameters explicit.) As expected from a dimensional analysis, η is independent of all parameters for the homogeneous chain, except n . In Fig. 1, we present a log-log plot of $(1 - \eta)$ versus n . For clarity, we only plot the range $n = 3$ to 50, but the same trend is evident to $n = 10^4$. Despite some oscillation, $(1 - \eta)$ fits very well a power law curve $An^{-\beta}$, with $A \approx 0.75$ and $\beta \approx 0.68$; and, extrapolating, one finds that $\eta \rightarrow 1$ as $n \rightarrow \infty$.

To gain insight into this result, we consider the details of the dynamics of a finite chain. Figure 2 shows the interaction of the $n = 9$, $k = 8$, homogeneous chain with the hard wall. First, we note that Δt_p and ν_p remains remarkably constant throughout the interaction, as can be seen in Fig. 3, where Δt_p and ν_p are plotted as a function of the collision number,

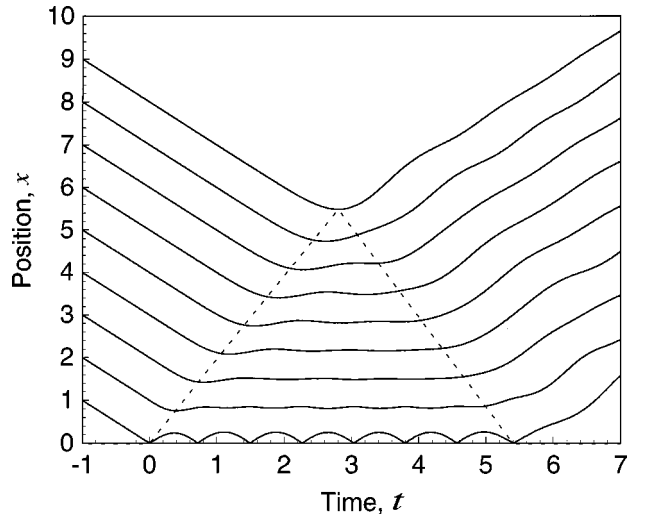


FIG. 2. The trajectories of the particles for the $n = 9$, $k = 8$, homogeneous chain. The dashed lines indicate the approximate division between the compressed and uncompressed regions. (Reduce units where $m = a = v_c = 1$.)

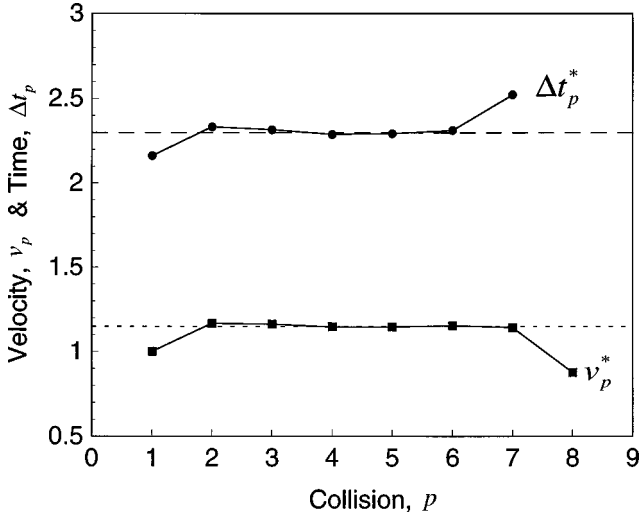


FIG. 3. The intercollision time intervals Δt_p and the collision velocity v_p as a function of collision number p for the $n=9, k=8$, homogeneous chain. The stars indicate reduced units $\Delta t_p^* = \Delta t_p / \sqrt{m/k}$ and $v_p^* = v_p / v_c$. The long and short dashed lines indicate the values of λ and κ , respectively.

p . As for longer chains, these only deviate significantly from their plateau values for the first and last collisions. The plateau values are themselves rather insensitive to n . From its value for $n=2$, where it can be shown that $\Delta t_p = \pi \sqrt{m/2k} \approx (2.2214) \sqrt{m/k}$, Δt_p gradually rises to $\lambda \sqrt{m/k}$, with $\lambda \approx 2.2995$; and similarly, v_p rises from v_c to κv_c , with $\kappa \approx \lambda/2 \approx 1.1498$, as $n \rightarrow \infty$. Further, we find that, the number of times particle $i=1$ collides with the wall is $f \approx n/\kappa \approx (0.8697)n$, and the time elapsed from the first to last collision is $T = t_p - t_1 \approx 2n \sqrt{m/k}$, as $n \rightarrow \infty$.

Next, we note in Fig. 2 that a well defined *front* separating the compressed from the uncompressed region of the chain propagates up and down it at the speed of sound in the medium $v_s = a \sqrt{k/m}$. (This is indicated with guidelines in Fig. 2.) This long wavelength (low frequency) excitation is evident in Fig. 4(a) where we plot $E_j^{(p)}$ for $p=0$ (before any collision) to $p=f=8$ (after the last). There, we see that most of the energy lost by the c.m. mode is acquired by the lowest frequency ($j=2$) mode during $0 \leq p \leq 4$, and redeposited into the c.m. mode during $4 \leq p \leq 8$. However, some of the energy does go into higher frequency modes, as is evident in Fig. 4(b). Still, as is the case for the $j=2$ mode, most of this energy is redeposited into the c.m. mode by the time the interaction ends, with $E_2^{(p)}$ having *almost* made one complete oscillation from $E=0$ and back, $E_3^{(p)}$ having *almost* made two, $E_4^{(p)}$ having *almost* made three, etc. This trend, however, breaks down for larger j as is already becoming apparent for $j=4$. Figure 5 shows the energy trapped in the internal modes after the last collision as a function of frequency for the $n=1001, k=1000$, homogeneous chain. We note that most of the “lost” energy resides in the lower frequency modes, in the approximate range $0 < \omega < n^{1/3} \sqrt{k/m}$.

More insight into the above results can be obtained if two simplifying assumptions are made in our analytical expressions. If we assume, in accordance with our numerical results, that $\Delta t_p = \Delta t$ and $v_p = v$ are constant for all p , then the mapping in Eq. (11) can be written in closed form, and Eq.

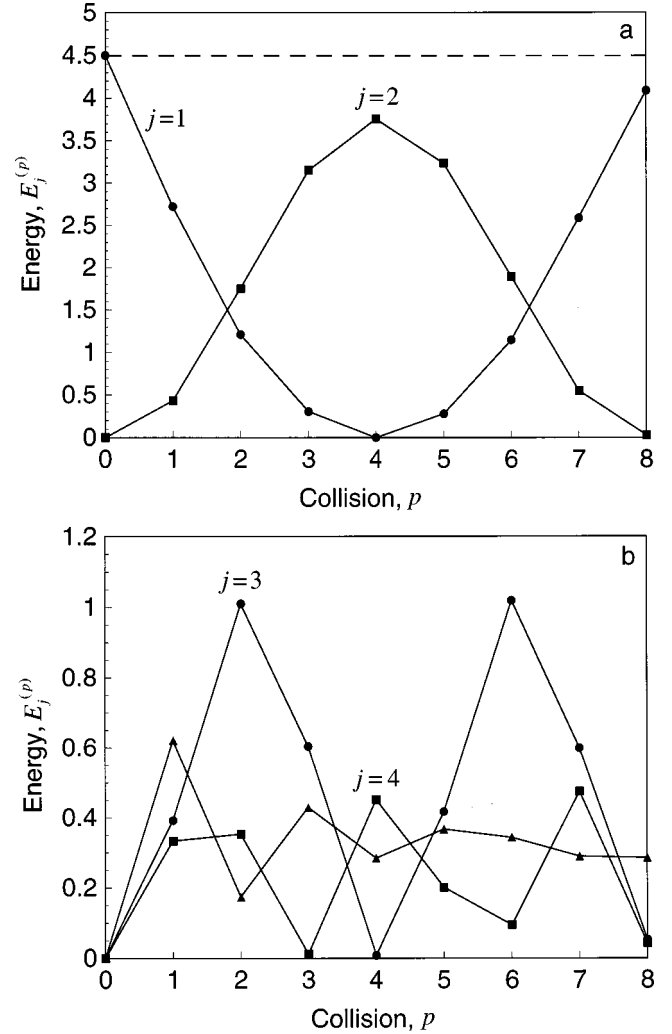


FIG. 4. (a) The energy in the c.m. mode (●) and in the lowest frequency mode (■) as a function of collision number p for the $n=9, k=8$, homogeneous chain. The dashed line indicates the total energy of the system. (b) The energy in the $j=3$ mode (●) and the $j=4$ modes (■) as a function of collision number, p , for the $n=9, k=8$, homogeneous chain. The energy in the remaining modes, $j=5, \dots, 9$ is summed (▲). (Reduced units where $m=a=v_c=1$.)

(7) yields an analytical expression for the energy in modes $j=2, 3, \dots, n$ after the p th collision:

$$E_j^{(p)} = \left(\frac{4m v^2}{n} \right) \left(1 - \frac{m \omega_j^2}{4k} \right) \frac{\sin^2(\omega_j p \Delta t / 2)}{\sin^2(\omega_j \Delta t / 2)}. \quad (14)$$

Similarly, ω_j has an analytical expression; but, since we expect $E_j^{(p)}$ to be largest for low frequencies, it is more instructive to substitute the Taylor expansion

$$\omega_j = \sqrt{k/m} \left(\frac{(j-1)\pi}{n} \right) \left\{ 1 - \frac{(j-1)^2 \pi^2}{24n^2} + O \left[\left(\frac{(j-1)}{n} \right)^4 \right] \right\}. \quad (15)$$

If only the leading order is retained, and we set $p=f$ and $f \Delta t = 2n \sqrt{m/k}$, then $E_j^{(f)} = 0$, for $j=2, 3, \dots, n$, with $E_j^{(p)}$ having performed *exactly* $(j-1)$ oscillations from $E=0$ and back. At this level of approximation, we have $\eta=1$, for any $n \geq 2$. We next retain the second order in Eq. (15) to obtain

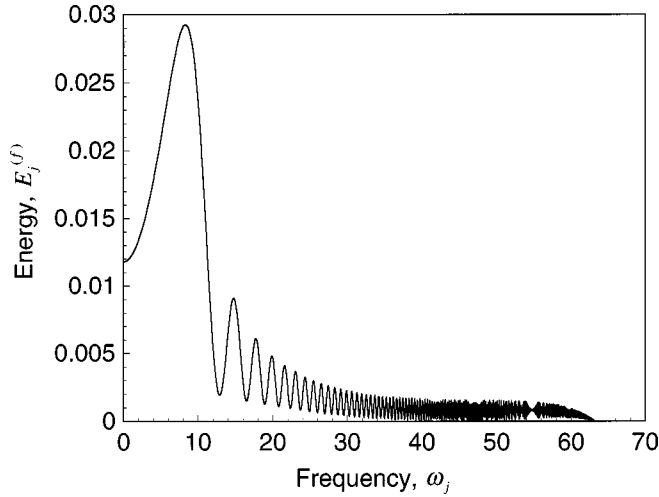


FIG. 5. The energy trapped in the internal modes, $E_j^{(f)}$, as a function of the mode frequency ω_j for the $n=1001$, $k=1000$, homogeneous chain. (Reduced units where $m=a=v_c=1$.)

the leading term in the asymptotic approach of η to 1. From the definition of η , we can write $1 - \eta = E_l/E_0$, where E_l is the “lost” energy which is given by $E_l = \sum_{j=2}^n E_j^{(f)}$. In the limit $n \rightarrow \infty$, this gives

$$1 - \eta \sim n^{-2/3} \left(\frac{16\kappa^2}{\pi\lambda^2} \right) \int_0^\infty [\sin^2(u^3/3)/u^2] du = An^{-\beta}, \quad (16)$$

with $A \approx 0.6522$ and $\beta = 2/3$, in good agreement with our numerics. (The value of the ratio, $\lambda/\kappa = 2$, can be derived from considerations of impulse.)

This analysis leads to the following picture: While the chain interacts with the wall, energy is exchanged between the c.m. mode and the internal modes in such a way that the energy in any particular mode j oscillates in time with the same natural frequency as the mode itself. Since most of the energy exchange occurs with the low frequency modes, and since these are almost commensurate in frequency, the total time the chain interacts with the wall is set by them. When the $j=2$ mode redeposits the last of its energy into the c.m. mode, the $j=3,4,5, \dots$, modes also redeposit theirs, the chain pushes away from the wall and the interaction ends. Thus, $E_2^{(p)}$ (almost) makes one complete oscillation, $E_3^{(p)}$ (almost) makes two, etc., giving the total interaction time $T \approx 2\pi/\omega_2 \approx 4\pi/\omega_3 \approx \dots \approx 2n\sqrt{m/k}$.

As a first order approximation, the above argument suffices to explain the overall dynamics; but, it does not explain the deviation of η from one for finite n , because, if all the internal modes were perfectly commensurate with one another, then one would have $\eta=1$, for any $n \geq 2$. Slight incommensurability in the frequencies, arising from higher order terms in ω_j , prevents all the energy distributed among the modes from being simultaneously redeposited—some energy must remain trapped in internal modes. While this “lost” energy increases with chain size as $n^{1/3}$, as a ratio to the total energy of the system, it decreases as $n^{-2/3}$, leading to the result that a homogeneous chain has $\eta=1$ in the thermodynamic limit.

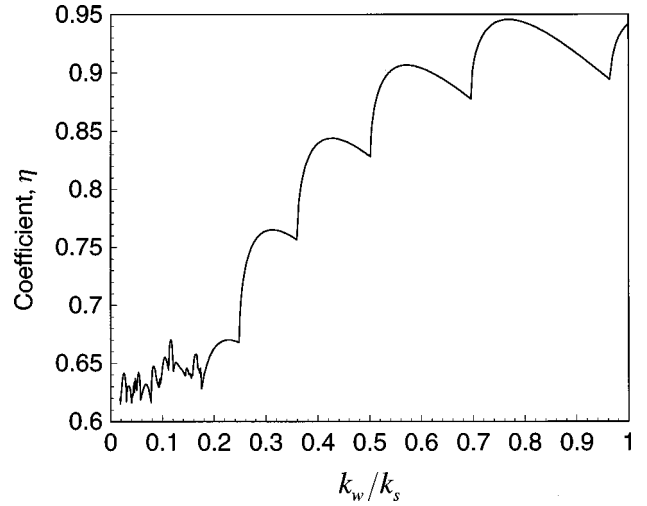


FIG. 6. The coefficient of elasticity η as a function of k_w/k_s for the $n=33$ cushioned chain. (Reduced units where $m=a=v_c=1$.)

IV. RESULTS FOR THE CUSHIONED CHAIN: HARD WALL COLLISIONS

It is clear from the analysis of the preceding section that, for η to remain significantly less than one in the thermodynamic limit, the dynamics of the homogeneous chain, in which most of the energy in the internal modes is simultaneously redeposited into the c.m. mode as the interaction ends, must be frustrated. In this section, we treat a particular chain which does so: the “cushioned” chain in which the colliding front half is made up of springs with constant k_w , the other half is made up of springs with constant k_s , and $k_w < k_s$. To keep the overall spring constant $K=1$, we insist that $1/k_w + 1/k_s = 2/(n-1)$, while varying k_w/k_s or n . In Fig. 6, we present η for the $n=33$ chain as a function of k_w/k_s . Despite some fluctuation, η generally decreases as the cushion is made softer and eventually deviates significantly from one. Furthermore, this deviation is not an artifact of the small chain size, but persists to larger sizes, as shown in Fig. 7 which presents η as a function of n with $k_w/k_s=0.2$ for $n=10$ to 1000.

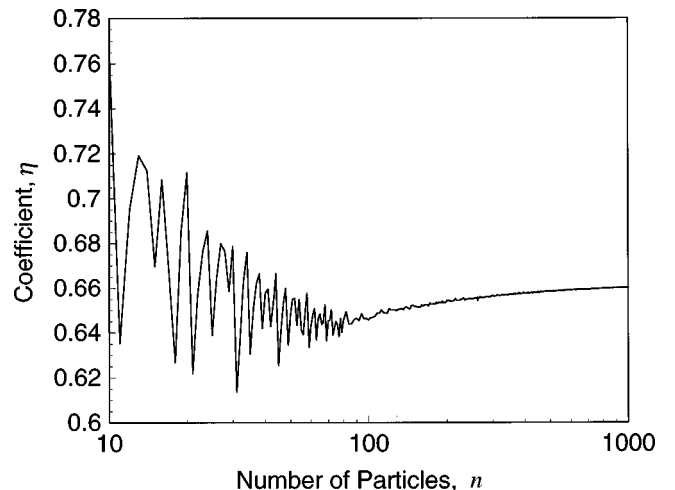


FIG. 7. The coefficient of elasticity η as a function of chain size, n , for the $k_w/k_s=0.2$ cushioned chain. (Reduced units where $m=a=v_c=1$.)

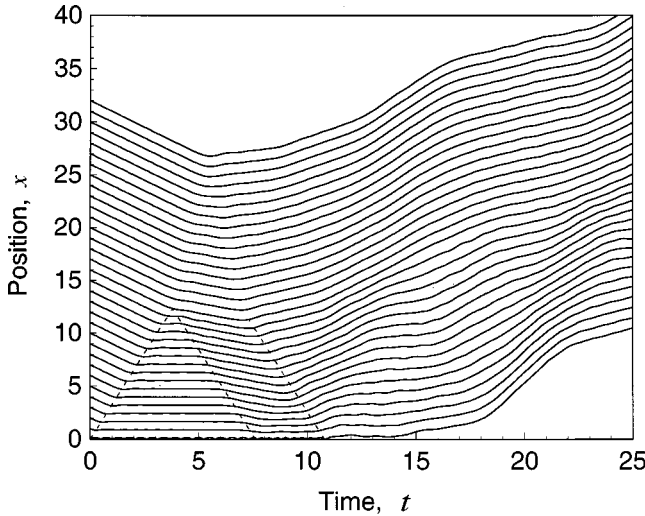


FIG. 8. The trajectories of the particles for the $n=33$, $k_w/k_s=0.2$, cushioned chain. The dashed lines indicate the approximate division between the variously compressed regions. (Reduced units where $m=a=v_c=1$.)

To gain insight into this result, we consider the $n=33$, $k_w/k_s=0.2$, cushioned chain. In Fig. 8, we plot the trajectories of the particles as the chain interacts with the wall, and in Fig. 9 we plot Δt_p and v_p as a function of collision number, p . We note two distinct phases to the dynamics.

(1) A homogeneouslike phase appears in Fig. 9, for $p=1$ to 13. In this phase, Δt_p and v_p exhibit the characteristic plateau behavior of a homogeneous chain with $k=k_w$. The corresponding feature in Fig. 8 is a front that propagates up and down the weaker half of the chain, traveling at the speed of sound in that region, $v_{sw}=a\sqrt{k_w/m}$, and ‘‘reflecting’’ off the interface between the two halves. For any cushioned chain with sufficiently small k_w/k_s , this phase lasts a time $T_w=n\sqrt{m/k_w}$, as $n\rightarrow\infty$.

(2) An over-compressed phase is evident in Fig. 9 where, for $p=14$ to 24, Δt_p decreases and v_p increases beyond their homogeneous values. It originates when the stiffer half of the

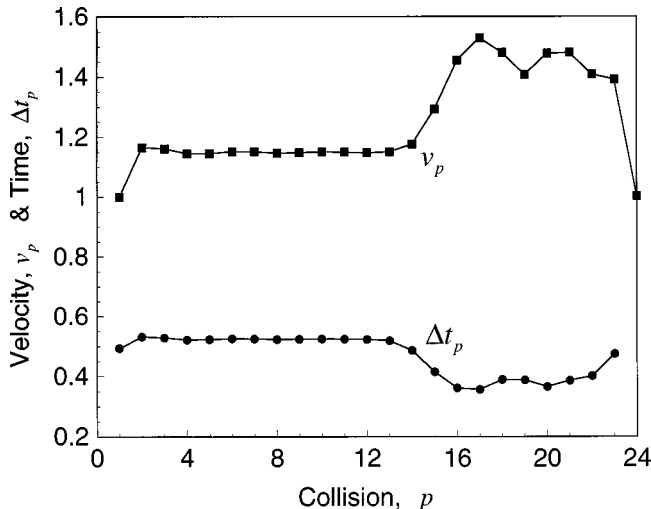


FIG. 9. The intercollision time intervals Δt_p and the collision velocity v_p as a function of collision number p for the $n=33$, $k_w/k_s=0.2$, cushioned chain. (Reduced units where $m=a=v_c=1$.)

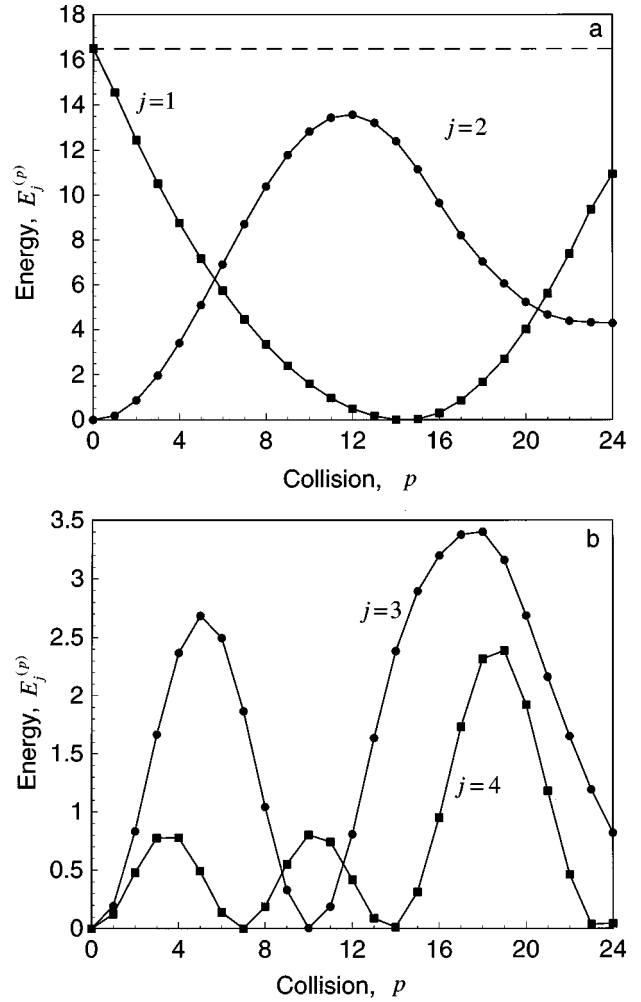


FIG. 10. (a) The energy in the c.m. mode (●) and in the lowest frequency mode (■) as a function of collision number p for the $n=33$, $k_w/k_s=0.2$, cushioned chain. The dashed line indicates the total energy of the system. (b) The energy in the $j=3$ mode (●) and the $j=4$ modes (■) as a function of collision number, p , for the $n=33$, $k_w/k_s=0.2$, cushioned chain. (Reduced units where $m=a=v_c=1$.)

chain collides into the weaker half. The reflected wave front propagates back through the weaker half causing further compression, beyond that of the homogeneouslike phase. This is seen in Fig. 8, where the various regions of different compression are indicated with guidelines. This phase ends when the interaction ends, and, for sufficiently small k_w/k_s , lasts a time $T_s=T_w/2$, as $n\rightarrow\infty$. Thus, the total interaction time is $T=(3n/2)\sqrt{m/k_w}$ for a sufficiently soft cushion and large chain.

Next, we plot $E_j^{(p)}$, for $j=1, 2, 3$, and 4, as a function of p in Fig. 10. We note the following (1) Most of the energy exchange during the interaction occurs between the c.m. mode and the lowest frequency mode. (2) Except for $j=2$, $E_j^{(p)}$ almost makes $(j-1)$ complete oscillations, although the amplitude is not constant throughout the interaction, and increases during the overcompressed phase. (3) $E_2^{(p)}$ does not complete one oscillation, not even approximately. It is this mode which is responsible for most of the ‘‘lost’’ energy for all sizes of cushioned chains with k_w/k_s sufficiently small. In Fig. 11, $E_j^{(f)}$ is plotted versus ω_j for the $n=33$, k_w/k_s

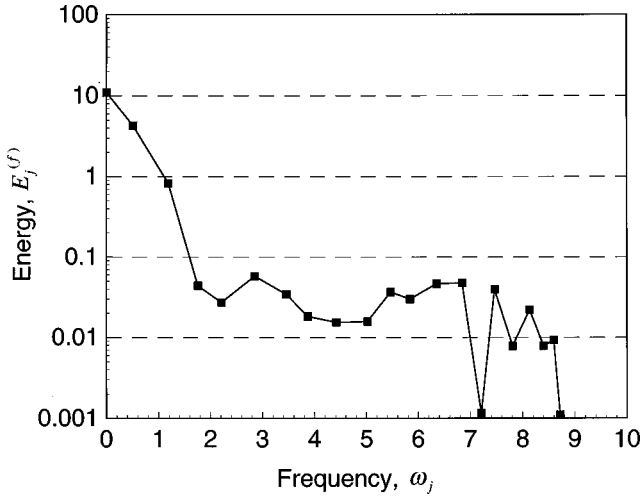


FIG. 11. The energy trapped in the internal modes $E_j^{(f)}$ as a function of the mode frequency ω_j for the $n=33$, $k_w/k_s=0.2$, cushioned chain. Only modes with energy greater than 0.001 are shown. (Reduced units where $m=a=v_c=1$.)

$=0.2$, cushioned chain. We see that $E_2^{(f)}$ is orders of magnitude larger than the energy trapped in the other modes.

These results can be understood as a frustration of the mechanism by which a homogeneous chain obtains $\eta=1$ in the thermodynamic limit. The deviation of Δt_p and ν_p from their plateau values during the overcompressed phase means that the advances in the phase of $C_j^{(p)}$ and the boost given to its amplitude with each successive collision [respectively, the first and second term in Eq. (11)], are no longer uniform and the closed form expression for $E_j^{(p)}$ in Eq. (14) is no longer valid. Rather, the loss in coherence of the phase advances and boosts results in more energy being trapped in various modes as the collision comes to an end. Since the lowest frequency modes acquire the bulk of the energy from the c.m. mode as the collision progresses, they are most susceptible to energy trapping. Although we illustrated this phenomenon here with the cushioned chain, we expect the same dynamics to occur in any chain in which there are interfaces between weaker and stiffer springs. Whenever the compression front reflects from such interfaces and returns to particle $i=1$, we expect further variations in Δt_p and ν_p , and further deviation from the coherence of the homogeneous chain, to occur.

V. SOFT WALL COLLISIONS

We next examine the opposite limit, namely collisions with a soft wall. We model such collisions by setting $H_I = \zeta x_1^2/2$ in Eq. (2), i.e., by putting particle $i=1$ of the chain in an external harmonic well. If $\zeta \ll k_i$ for all i , then a collision of particle $i=1$ with the left or right wall of the well is very slow compared to internal vibrations. In particular, the internal vibrations of the chain are given plenty of time to respond to a collision with the left wall before a collision with the right wall occurs. In this way, we can consider an isolated collision of the chain with the left wall.

Note that only particle $i=1$ in the chain feels the force of the wall, even though the wall has an effective thickness larger than the chain length in the $\zeta \rightarrow 0^+$ limit. This is in

keeping with our view of collisions wherein interaction with the wall is restricted to the interface, and the collision is communicated to the bulk of the chain via successive internal interactions. The model, as modified in this section, retains this feature while allowing the interaction with the wall to appear very gradually: $\zeta \rightarrow 0^+$ is an adiabatic limit, in contrast to the sudden limit of hard wall collisions.

With H_I set as above, \mathbf{K} has the same form as in Eq. (4), except that $k_0 = \zeta$. We will signify such modifications by a prime superscript, e.g., \mathbf{K} becomes \mathbf{K}' . To see how the soft wall collisions work, we diagonalize \mathbf{K}' for small ζ using perturbation theory. Here, the perturbation is ζ/m in the (1,1) component of the matrix. In first order perturbation theory, the perturbed eigenvalues $(\omega'_j)^2$ are given by

$$(\omega'_j)^2 = \omega_j^2 + \frac{\zeta}{m} (\hat{g} \cdot \hat{e}_j)^2, \quad (17)$$

and the eigenvectors do not change at all. In the case of a homogeneous chain, the forms of ω_j and $(\hat{g} \cdot \hat{e}_j)^2$ have analytical expressions; however, ω'_1 can be evaluated without restriction to the homogeneous case $\omega'_1 = \sqrt{\zeta/nm}$, for all chains.

The advantage of this variation on the model is that the dynamics is entirely harmonic, and the collision appears entirely within the framework of harmonic dynamics. To see how this works, consider the c.m. degree of freedom which in this version of the model is no longer associated with zero frequency; however, since ζ is small, the c.m. frequency is small and the associated period is large. A complete collision then corresponds to a half period of the c.m. oscillation, and inelasticity of the collision corresponds to energy transfer from the c.m. motion to the other degrees of freedom during the course of this half period. However, to first order in ζ , the c.m. degree of freedom corresponds exactly to a normal mode of the harmonic oscillator; thus, the c.m. energy is a constant of the motion at this level of approximation, and the collision is perfectly elastic. This is true for any set of k_i , and does not depend on the thermodynamic limit. In contrast to a hard wall collision, a very soft wall collision is rather insensitive to the characteristics of the harmonic chain.

To get an inelastic soft wall collision, we must go to second order perturbation theory. At this level, the eigenvector \hat{e}'_1 is perturbed away from the c.m. degree of freedom, while the other eigenvectors pick up small components of c.m. motion. In second order perturbation theory (i.e., eigenvalues given to second order), the corrections of the eigenvectors are first order in ζ . Specifically,

$$\hat{e}'_j = \hat{e}_j + \frac{\zeta}{m} \sum_{k \neq j} \frac{(\hat{g} \cdot \hat{e}_j)(\hat{g} \cdot \hat{e}_k)}{\omega_j^2 - \omega_k^2}. \quad (18)$$

Although this eigenvector is not normalized, it can be used as it stands because the leading correction to achieve normalization is second order in ζ .

The time evolved chain configuration still is given by Eqs. (5) and (6), except that primed quantities replace unprimed ones. Because the dynamics is purely harmonic, C'_j does not change with time. The outcome of the collision is thus determined transparently in terms of the initial conditions which we use to evaluate C'_j . With perturbed eigenvectors,

the initial conditions are not as in the original model, wherein $C_j = -i\nu_c\sqrt{n}$, for $j=1$, and zero otherwise. Rather, using the same initial state of the chain as above (i.e., pure c.m. motion heading towards the left wall), we have that $C'_j = -i\nu_c\hat{e}_1 \cdot \hat{e}'_j$.

Thus, an initial excitation of the c.m. degree of freedom now corresponds to excitation of all the normal modes, although all C'_j but C'_1 are small. Using Eq. (18), we can evaluate C'_j :

$$C'_j = -i\nu_c \left[\delta_{j,1} + (1 - \delta_{j,1}) \frac{\zeta}{m\sqrt{n}} \frac{\hat{g} \cdot \hat{e}_j}{\omega_j^2} \right]. \quad (19)$$

The same expression for C'_j applies before, during and after the collision with the soft wall. To see how inelasticity emerges, reconsider the initial state of the chain. It is a linear combination of all normal modes, the same linear combination at all times. However, initially the normal modes are phased such that this linear combination produces motion only in the c.m. degree of freedom. At later times, the phase alignment is destroyed and internal vibrations are excited. A complete collision requires half a period of the $j=1$ mode, which corresponds to many periods of the other modes. Thus, we can expect the phases of the $j=2,3,\dots,n$ modes to be, in a sense, randomized at the end of the collision.

At this stage it is convenient to consider the thermodynamic limit $n \rightarrow \infty$. In this limit, all but the $j=1$ mode are spread out over very many degrees of freedom, and the c.m. motion represents a negligible component of any one of these modes. The total energy in all modes, but $j=1$, can thus be interpreted as the total energy in the internal degrees of freedom at the end of the collision. Only here, the total energy in the $j=2,3,\dots,n$ modes is independent of time, and it just happens that the energy is manifest as c.m. motion initially. At the end of the collision, the modes are randomly phased and the energy is lost from c.m. motion.

We can now evaluate the coefficient of restitution using $1 - \eta = E_1/E_0$:

$$1 - \eta = \left(\sum_{j=2}^n \frac{m}{2} |C'_j|^2 \right) / \left(\frac{m}{2} |C'_1|^2 \right) = \frac{\zeta^2}{m^2 n} \sum_{j=2}^n \frac{(\hat{g} \cdot \hat{e}_j)^2}{\omega_j^4}. \quad (20)$$

In the case of a homogeneous chain, this yields an analytical expression with a simple form in the limit $n \rightarrow \infty$:

$$1 - \eta \sim \frac{\zeta^2}{4\pi k^2 n} \int_{\pi/2n}^1 (\sqrt{1-z^2}/z^4) dz = \frac{2\zeta^2 n^2}{3\pi^4 k^2}. \quad (21)$$

Equation (21) gives the leading term in the thermodynamic limit. The last expression is understood by first noting that the adiabatic limit, which we use to define a soft collision, must be taken before the thermodynamic limit. More specific to Eq. (21), this means that ζ must be small compared to k/n . This ensures that the collision interaction is slower than the lowest frequency vibrations; otherwise, the use of perturbation theory is inappropriate.

Equation (21) shows how elasticity is approached in the adiabatic limit (i.e., as ζ^2) while revealing the curious result

that inelasticity actually increases with increasing n in soft wall collisions, quite at odds with the elasticity of hard wall collisions of homogeneous chains in the thermodynamic limit. The increasing inelasticity results because of the denominator in Eq. (18). In the thermodynamic limit there are modes with arbitrarily low frequency. These modes interact most strongly with the zeroth order $j=1$ mode, which represents pure c.m. motion, and they yield large contributions to the inelasticity. Since the profusion of low frequency modes occurs for all chains in the thermodynamic limit, not just homogeneous chains, we expect growth in inelasticity for all chains as $n \rightarrow \infty$.

VI. CONCLUDING REMARKS

While simple in nature, our model does give considerable insight into how energy is lost to the internal degrees of freedom of a solid during inelastic collisions where the microscopic forces involved are purely conservative. For a homogeneous chain colliding with a hard wall, energy originally in the c.m. mode is distributed among the internal modes as the collision progresses, but this energy is effectively redeposited into the c.m. mode simultaneously as the interaction ends, giving a coefficient of restitution near unity. This process is seen as the propagation of a compression front through the chain, with near perfect transmission of the energy back into c.m. motion when the front reaches the end of the chain.

For an inhomogeneous chain colliding with a hard wall, energy is again distributed among the modes. However, boundaries between regions with different force constants reflect the compression front and this gives rise to a loss in phasing of the modes in comparison with the homogeneous chain. As a result, at the end of the interaction, more energy is trapped in some modes and the chain is considerably less elastic.

In contrast to collisions with a hard wall, soft wall collisions are always perfectly elastic in the adiabatic limit, despite the details of the spring constants connecting the masses. Also, unlike hard wall collisions, the asymptotically small inelasticity associated with soft wall collisions increases with chain size— asymptotically small with respect to collision adiabaticity.

Not surprisingly the most important modes involved in the restitution are the low frequency modes, i.e., the “bulky” modes of long wavelength. The higher frequency modes play a minimal role in both homogeneous and inhomogeneous chains. Our model, then, does not really demonstrate how energy is dissipated into heat, in which the energy is more or less equally distributed among all the modes according to the equipartition theorem. This ultimate arrangement of internal energy results only with inclusion of anharmonic terms in the interparticle potential which would couple the normal modes and allow energy to leak to higher frequency modes over time. However, at least at low collision velocity for which anharmonicity is a small perturbation, the thermalization of internal energy can be viewed as subsequent to the collision-induced energy rearrangement we investigate.

- [1] C. L. Cleveland and U. Landman, *Science* **257**, 355 (1992).
- [2] T. Raz and R. D. Levine, *J. Chem. Phys.* **105**, 8097 (1996).
- [3] W. Christen, U. Even, T. Raz, and R. D. Levine, *J. Chem. Phys.* **108**, 10 262 (1998).
- [4] P. U. Andersson and J. B. C. Pettersson, *J. Phys. Chem. B* **102**, 7428 (1998).
- [5] C. E. Smith and P. Liu, *J. Appl. Mech.* **59**, 963 (1992).
- [6] For example, see C. Thornton, *J. Appl. Mech.* **64**, 384 (1997); C. Thornton, Z. Ning, *Proceedings of the 1st International Particle Technology Forum* (AIChE, New York, 1994), Vol. II, p. 14.
- [7] The model of the homogenous chain treated here does not make the simplifying assumptions characteristic of standard textbook presentations. They treat the homogeneous chain either (1) with particles $i=1$ and n fixed to their equilibrium position, see T. C. Bradbury, *Mathematical Methods* (Wiley, New York, 1984), pp. 337-341 or (2) with Born-von Karman boundary conditions, see C. Kittel, *Introduction to Solid State Physics*, 7th ed. (Wiley, New York, 1996), pp. 99-100. While these simplify the math, they also remove modes crucial to our analysis.
- [8] The problem of finding the time intervals, Δt_{p-1} , is the problem of finding ‘‘gap times’’ in the harmonic approximation of the theory of unimolecular reactions. See N. B. Slater, *Theory of Unimolecular Reactions* (Cornell University Press, Ithaca, NY, 1959), Sec. 9.6, p. 206.
- [9] H. Gould and J. Tobochnik, *An Introduction to Computer Simulation Methods* (Addison-Wesley, New York, 1988), Part I, pp. 107-112.